MPMI Vol. 18, No. 11, 2005, pp. 1161–1174. DOI: 10.1094/MPMI-18-1161. © 2005 The American Phytopathological Society

*e*-Xtra*

# Expression Profiling Soybean Response to *Pseudomonas syringae* Reveals New Defense-Related Genes and Rapid HR-Specific Downregulation of Photosynthesis

**Jijun Zou,[1] Sandra Rodriguez-Zas,[2] Mihai Aldea,[3] Min Li,[1] Jin Zhu,[1] Delkin O. Gonzalez,[1] Lila O. Vodkin,[1] Evan DeLucia,[3] Steven J. Clough[1,4]**

[1]Department of Crop Sciences, University of Illinois; [2]Department of Animal Sciences, University of Illinois; [3]Department of Plant Biology, University of Illinois, Urbana, IL 61801, U.S.A.; [4]USDA-ARS, Urbana, IL 61801, U.S.A.

Submitted 3 March 2005. Accepted 14 July 2005.

**Transcript profiling during susceptible (S) and hypersensitive response–associated resistance (R) interactions was determined in soybean (*Glycine max*). *Pseudomonas syringae* pv. *glycinea* carrying or lacking the avirulence gene *avrB*, was infiltrated into cultivar Williams 82. Leaf RNA was sampled at 2, 8, and 24 h postinoculation (hpi). Significant changes in transcript abundance were observed for 3,897 genes during the experiment at $P \leq 0.000005$. Many of the genes showed a similar direction of increase or decrease in abundance in both the S and R responses, but the R response generally showed a significantly greater degree of differential expression. More than 25% of these responsive genes had not been previously reported as being associated with pathogen interactions, as 704 had no functional annotation and 378 had no homolog in National Center for Biotechnology Information databases. The highest number of transcriptional changes was noted at 8 hpi, including the downregulation of 94 chloroplast-associated genes specific to the R response. Photosynthetic measurements were consistent with an R-specific reduction in photosystem II operating efficiency ($\Phi_{PSII}$) that was apparent at 8 hpi for the R response with little effect in the S or control treatments. Imaging analyses suggest that the decreased $\Phi_{PSII}$ was a result of physical damage to PSII reaction centers.**

*Additional keywords*: compatible, genomic, incompatible, oxidative burst.

Plants have evolved resistance (*R*) genes that recognize the presence of avirulent (*avr*) gene products released by bacterial, fungal, and viral pathogens (Bonas and Lahaye 2002). This specific but sometimes indirect (Rooney et al. 2005) recognition triggers a rapid, incompatibility resistance response that results in rapid production of antimicrobial compounds, such as reactive oxygen species (ROS), catabolic enzymes, and toxic chemicals, effectively putting an end to pathogen invasion and preventing further disease development (Doke 1983; Hammond-Kosack and Jones 2000; Mahalingam and Fedoroff 2003). If the attacked plant lacks a specific *R* gene capable of recognizing the presence of an Avr protein from the pathogen, the signaling of defenses may be less rapid and less robust, allowing the pathogen greater opportunity to overcome the defenses and possibly lead to a susceptible interaction and disease development (Lamb and Dixon 1997; Tao et al. 2003). Successful triggering of the incompatible resistance reaction may lead to the hypersensitive response (HR) and programmed cell death (PCD); however, mutation in the gene *DND1* (ion-channel CNGC2) has shown that it is possible for plants to activate an incompatible resistance response in an *avr/R* gene–specific manner without provoking PCD (Clough et al. 2000; Yu et al. 1998). Likewise, the *R* gene *Rx* in potato specifically recognizes potato virus X coat protein to induce rapid resistance without HR-associated PCD (Bendahmane et al. 1999).

Although the *Arabidopsis thaliana–Pseudomonas syringae* interaction has been a model system to study plant-pathogen molecular interactions (Quirino and Bent 2003), some of the first molecular studies on plant-pathogen interactions involved *P. syringae* and the plant host soybean (*Glycine max*). For example, the first *avr* gene to be cloned from any plant pathogen was *avrA*, isolated from *P. syringae* pv. *glycinea* based on differential interactions on several soybean cultivars (Staskawicz et al. 1984). The cloning of two additional *P. syringae* pv. *glycinea* genes that induced avirulence on soybean, *avrB* and *avrC*, quickly followed (Napoli and Staskawicz 1987; Staskawicz et al. 1987; Tamaki et al. 1988).

The genome sequence of *P. syringae* suggests approximately 50 or more secreted proteins that may serve as potential avirulence factors on various hosts. Interestingly, several avirulence factors have been proven to be associated with pathogen fitness functions and enhanced virulence when not efficiently recognized by the host defense system (Chen et al. 2004; Jamir et al. 2004; Kearney and Staskawicz 1990; Vivian and Gibbon 1997). Cognate resistance gene partners have been identified between *P. syringae* pv. *glycinea avr* genes and soybean *R* genes. *P. syringae* pv. *glycinea* carrying *avrA* provokes an HR on soybean lines carrying dominant *RPG2* (Ludwig and Tenhaken 2000, 2001; Seehaus and Tenhaken 1998), whereas *avrB* provokes HR if paired with *RPG1* (Ashfield et al. 1995;

Corresponding author: S. J. Clough; E-mail: sjclough@uiuc.edu

Upon request, all novel materials described in this publication will be made available in a timely manner for noncommercial research purposes. Nucleotide sequence data is available in the NCBI Gene Expression Omnibus (GEO) database as accession number GSE2961.

*The ***e***-Xtra logo stands for "electronic extra" and indicates the HTML abstract available on-line contains 11 supplemental tables not included in the print edition.

Staskawicz et al. 1987), the first resistance gene to be cloned from soybean (Ashfield et al. 2004).

Plant microarrays allow for the analysis of tens of thousands of genes simultaneously and can provide an insight into gene induction during a pathogen attack (Wan et al. 2002). Examining transcriptional response to *P. syringae*, Scheideler and associates (2002) used cDNA arrays comprising 13,000 unique expressed sequence tags (EST) to examine the transcriptional changes occurring during the interactions between *A. thaliana* and *P. syringae* pv. *tomato* carrying the avirulence gene *avrRpt2*. Tao and associates (2003) monitored approximately 8,000 genes for expression change in *A. thaliana* for response to *P. syringae* and suggested that, on a genome-wide scale, the HR induces genes more robustly and more rapidly than those induced during infection with compatible, virulent strains.

Many of the tools of the plant genomic era were developed originally in the model plant *A. thaliana*. However, genomic tools are available today for the study of economically important crop plants such as soybean, an agro-ecosystem that occupies approximately 30 million hectares in the United States and has an approximate value of $18 billion (United States Department of Agriculture 2001). Large-scale transcript profiling comparisons between susceptible and HR-associated resistance in soybean to *P. syringae* pv. *glycinea* or any other pathogen can now be determined. We used soybean cDNA microarrays (Vodkin et al. 2004) to assay the differential expression of 27,648 genes in HR-associated resistant (R) versus susceptible (S) responses by monitoring transcript levels in soybean inoculated with *P. syringae* pv. *glycinea* carrying or lacking *avrB*.

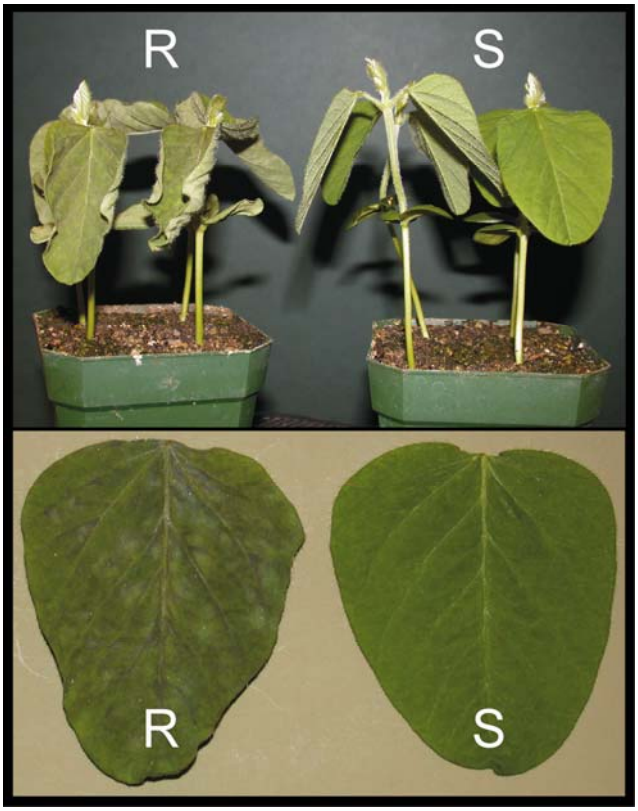


**Fig. 1.** Symptoms at 24 h postinoculation (hpi) in plants inoculated with *Pseudomonas syringae* carrying or lacking *avrB*. The hypersensitive response–associated resistance (R) response was induced in the leaf tissue and cotyledons. Plants inoculated with a virulent strain of *P. syringae* lacking *avrB* were susceptible (S) and showed no obvious symptoms within 24 hpi. Similar results have been previously reported (Ashfield et al. 1995). The slight epinasty was due to the handling of plants during photographing.

Our analysis indicates that differences between R and S responses reflect quantitative differences in the levels of thousands of gene transcripts, thus identifying a putative defense role for many of them, including several hundred that have no current functional annotation. Furthermore, our data support that photoinhibition may contribute to the HR-associated R response. Nearly 100 putative nuclear-encoded chloroplast genes were specifically down-regulated, and fluorescence measurements indicated a corresponding downregulation of photosystem II (PSII) operating efficiency and an increase in nonphotochemical quenching during the HR-associated R response.

Defense to a pathogen has been characterized as involving three phases: induction, effector, and degradation (Jabs 1999). The induction stage (Phase I) involves the priming of defenses and is associated with an initial short-lived, weak oxidative burst that can be induced by a wide variety of stresses involving nonspecific biotic and abiotic elicitors. The effector stage (Phase II) modulates the response to the initial stress by reducing or amplifying signals, such as the production of an additional, stronger, secondary oxidative burst that is specific to HR-associated R interactions, leading to (or not) Phase III, degradation in the form of PCD, which is postulated to occur only if sufficient defense signaling events have transpired during the first two phases. In soybean, Phase I occurs during the first 2 h following association with a pathogen and Phase II begins at about 3 h postinoculation (hpi) and lasts until about 10 hpi or longer (Lamb and Dixon 1997). Phase III occurs by 24 hpi and is accompanied by dark brown pigmentation and necrosis (Ashfield et al. 1995). Therefore, to compare soybean response to both S and HR-associated R reactions, we assayed leaf transcript levels at timepoints 2, 8, and 24 hpi (also referred to as samples T2, T8, and T24 respectively).

## RESULTS

### Symptom development.

To maximize the number of plant cells in contact with the bacteria, leaves were vacuum-infiltrated with inoculum. We

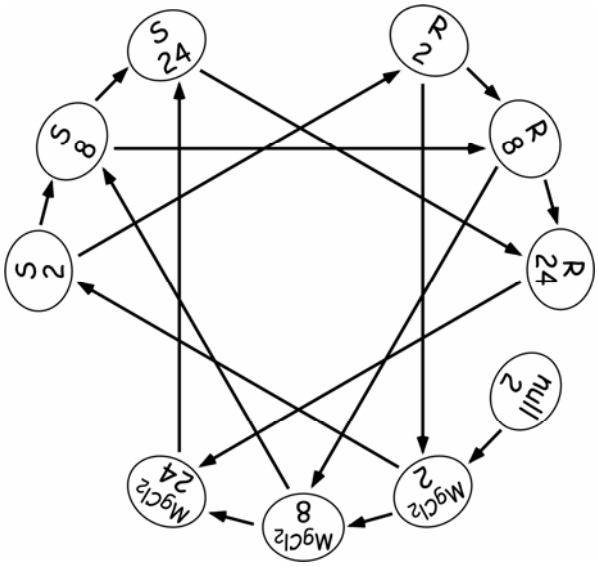


**Fig. 2.** Loop design used in microarray studies. Each arrow represents one microarray slide and connects the two individual samples hybridized to it. A total of 14 hybridizations involving 10 samples from different timepoints and treatments were used in this study for each of three cDNA libraries. R = resistant, leaves infiltrated with *Pseudomonas syringae* pv. *glycinea* carrying *avrB*, S = susceptible, leaves infiltrated with *P. syringae* pv. *glycinea* lacking *avrB*, $MgCl_2$ = leaves infiltrated with 10 mM $MgCl_2$ solution. The numbers in the circles indicate hours postinoculation.

observed that the pairing of *RPG1* and *avrB* induced an HR-associated R response, as evident by browning and necrosis of the leaf tissue within 24 h (Fig. 1) similar to that reported earlier (Ashfield et al. 1995). However, it should be noted that the R response did not lead to complete death of the entire leaf tissue within 24 hpi. Much of the leaf tissue remained green and did not entirely collapse (Fig. 1). In contrast, in the S interactions, in which *avrB* was not present, as well as in control plants infiltrated with 10 mM $MgCl_2$, no symptoms were observed within 24 hpi (Fig. 1). No visible symptoms were present at 2 or 8 hpi for any of the three treatments.

**Identification of 3,897 differentially expressed genes throughout the experiment.**

The experimental design (Fig. 2) and statistical data analysis provided a *P* value corresponding to the significance of the differential expression of each gene during the entire experiment as well as during pair-wise comparisons of any two specific treatments within the experiment. Therefore, to generate lists of significantly differentially expressed genes, we utilized two selection criteria. The first criterion was a *P* value less than 0.000005 over the entire experiment, equivalent to an experiment-wide false-discovery rate (FDR) of 0.138 (27,684 spots × 0.000005). This criterion allowed for selection of 3,897 genes, of the 27,684 screened, as being significantly differentially expressed during the course of the experiment. Secondly, we set a *P* value cutoff of 0.0001 for the specific pair-wise comparison of the treatments. Only genes that met both criteria, overall $P < 0.000005$ and specific comparison $P \leq 0.0001$, were deemed significantly differentially expressed.

**Common stress response among T2 samples.**

Vacuum infiltration water-soaked the leaves and therefore exposed a high number of plant cells to inoculum, but it also elicited an effect on gene transcription. Comparing T2 $MgCl_2$-infiltrated samples to T2 null (untouched) control plants that were not inoculated or subjected to vacuum infiltration revealed that 172 gene transcripts ($P \leq 0.0001$) were significantly altered in abundance at 2 hpi by the stress of infiltration (Fig. 3A). Interestingly, most of the identified gene transcripts were increased (95%), with only 5% reduced in abundance. More than one fourth of these genes were undefined, as their sequences either failed to find a homologous hit or were homologous to genes annotated as 'unknown'. The top categories (ignoring unknown, miscellaneous, and no hits) showing significant transcript increase and listed in order of frequency were: signaling, primary metabolism, DNA/RNA, defense, membrane, stress, protein, and cell wall and development. Genes included were putative calmodulins (AI460551, AW278834, and AI437703), calcium-dependent protein kinase (AW432503), WRKY family transcription factors (AW133440, AW396234, AW459004, BE021550, and AW458543), AP2-related transcription factor (AW233956), peroxidases (AW666030, AI442651, and AW278321), leucine-rich repeat (LRR)-types (AW756306, AI973594, and AW234414), and a 14-3-3-like protein (AI965330).

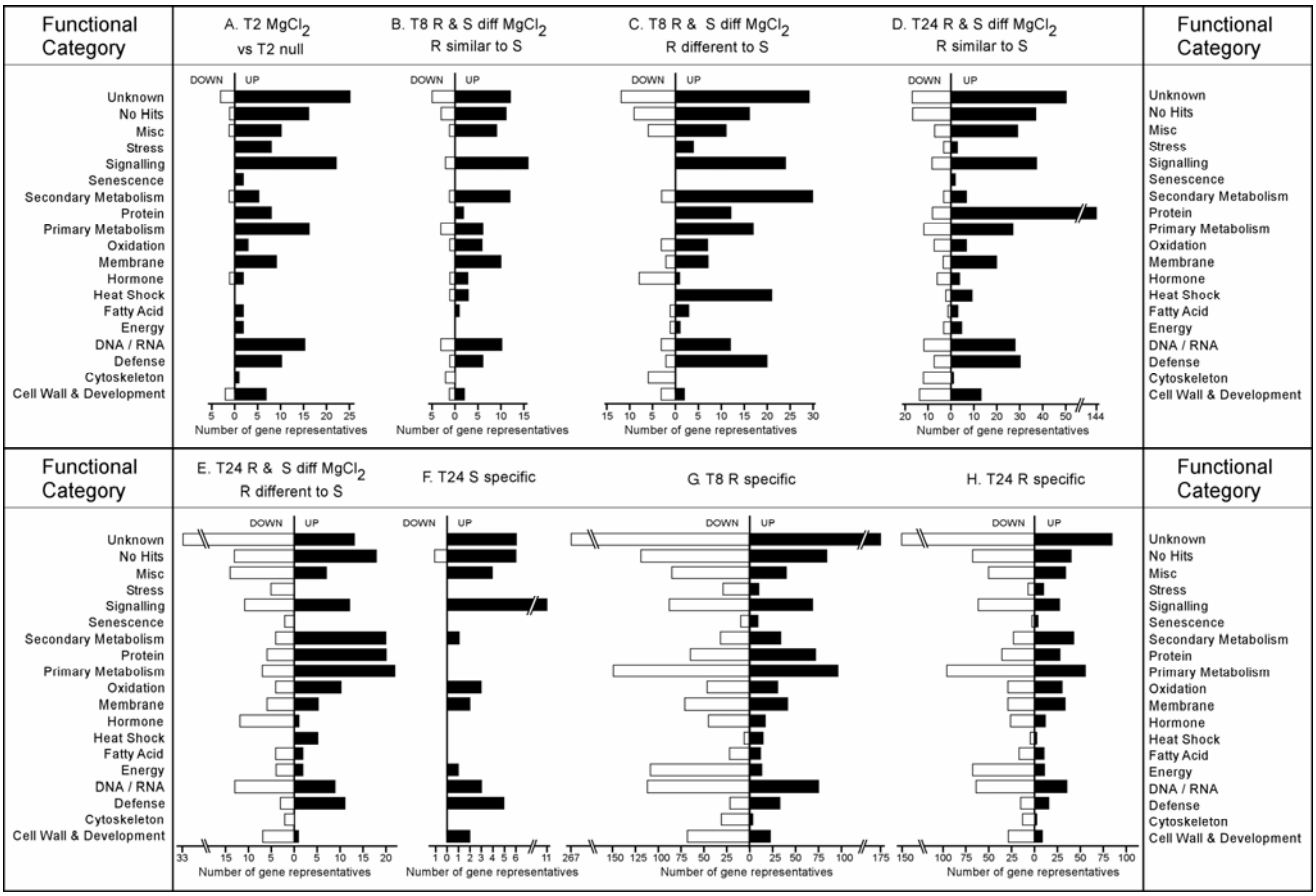


**Fig. 3.** Bar graphs indicating relative number of differentially expressed genes. Black bars indicate the number of genes whose RNA levels were significantly increased and white bars indicate decrease in abundance. R = hyprsensitive response–associated resistance, S = susceptible response. **A,** T2 $MgCl_2$ versus T2 null. **B,** R and S are significantly different from $MgCl_2$, but R is not significantly different from S. **C,** R and S are significantly different from $MgCl_2$, and R is significantly different from S. **D,** R and S are significantly different from $MgCl_2$, but R is not significantly different from S. **E,** R and S are significantly different from $MgCl_2$, and R is significantly different from S. **F,** S is significantly different from R and $MgCl_2$. **G,** R is significantly different from S and $MgCl_2$. **H,** R is significantly different from S and $MgCl_2$.

**Phase I: R- and S-specific expression.**

It was difficult to identify genes specifically altered by the bacterial pathogens in the T2 samples using the *P* value cutoff of 0.0001. In addition to the effects of infiltration on gene expression at this early timepoint, few cells would be responding to *P. syringae* pv. *glycinea* as the molecular interactions were just beginning to take place. Therefore, transcripts of only one gene (AW119629, no hit) were detected as being significantly increased at a $P \leq 0.0001$ in RNA abundance in R versus the control, and only one gene transcript (AW306798, partially homologous to a fructokinase, up in abundance) was significantly differentially expressed in S versus control. To identify the most likely gene candidates whose transcript levels were affected specifically by the bacterial pathogens during Phase I of the interactions, when these transcript changes were more subtle, it was necessary to lower the criterion of selection to a $P \leq 0.005$. At this significance level, 52 gene transcripts were increased or reduced in the S but not the R interaction, whereas 27 gene transcript levels were altered in R but not in S, and 11 genes were identified as being altered in abundance in both R and S compared with the $MgCl_2$ control. The results revealed a higher abundance of RNA homologous to genes encoding heat-shock proteins in both R and S than the $MgCl_2$-infiltration control. Also noted was a greater abundance of five glutathione *S*-transferase (GST) sequences (AW704357, AW508224, BE019990, AW100840, and AI441991) in the S than in the R samples.

**Phase II and III: Similar (but quantitatively different) expression trend between R and S responses.**

Tao and associates (2003) noticed that the difference in genomic responses to virulent and avirulent pathogens in *A. thaliana* was quantitative. A given gene tended to be induced

**Table 1.** Chloroplast related genes showing significant difference in RNA abundance in resistant (R) vs. susceptible (S) at 8 hpi

| GenBank ID | Annotation | Fold change[a] | *P* value[b] |
|---|---|---|---|
| Down-regulated in R at T8 | | | |
| AW569121 | 3-Oxoacyl-[acyl-carrier-protein] reductase | –1.78 | 6.41E-07 |
| AI855689 | Anthranilate phosphoribosyltransferase | –1.40 | 1.42E-06 |
| AI460948 | APG (AlbinoPaleGreen) mutant Plastiquinone biosyn | –1.08 | 9.14E-06 |
| AW396010 | ATP synthase B′ chain | –1.26 | 1.92E-06 |
| AW186038 | ATP synthase gamma chain | –2.44 | 2.33E-08 |
| AW132325 | Carotene biosynthesis-related protein CBR | –2.38 | 7.41E-09 |
| AW568620 | Chlorophyll a/b-binding protein | –2.31 | 2.97E-09 |
| AW101776 | Chlorophyll a/b-binding protein (cab-11) | –2.57 | 5.66E-08 |
| AW472547 | Chlorophyll a/b-binding protein (LHCII type III) | –2.82 | 2.68E-09 |
| AW100823 | Chlorophyll a/b-binding protein (photosystem I, type II) | –1.69 | 1.47E-08 |
| AW133329 | Chlorophyll a/b-binding protein (photosystem II, type I) | –1.69 | 6.78E-08 |
| AI736217 | Chlorophyll a/b-binding protein CP24 | –2.57 | 7.36E-09 |
| AI437691 | Chlorophyll a/b-binding protein CP29 | –2.60 | 9.21E-10 |
| AW423489 | Chlorophyll a/b-binding protein type I | –2.03 | 5.82E-10 |
| AI736285 | Chlorophyll a/b-binding protein type II | –2.43 | 5.95E-07 |
| AW201734 | Chlorophyll a/b-binding protein, PSI type III | –2.41 | 9.65E-07 |
| AW133138 | Chlorophyll A-B binding protein 3 | –1.44 | 6.71E-08 |
| AW459297 | Chlorophyll b synthase | –2.41 | 3.12E-08 |
| AI437592 | Chlorophyll oxidoreductase | –3.07 | 4.28E-12 |
| AI959779 | CP12 protein precursor | –1.88 | 3.08E-06 |
| AW831889 | Cytochrome b | –0.66 | 1.63E-08 |
| AI494909 | Cytochrome B6-F complex iron-sulfur subunit | –1.33 | 1.38E-08 |
| AW099343 | DAG protein | –0.72 | 5.7E-06 |
| AW707242 | Delta-aminolevulinic acid dehydratase | –1.10 | 1.09E-05 |
| AI495852 | DNA binding protein (CND41) | –1.21 | 1.43E-05 |
| AI736890 | Ferredoxin | –2.32 | 1.47E-09 |
| AI794970 | Ferredoxin--NADP+ reductase | –1.29 | 1.02E-09 |
| AW831184 | Fructose-bisphosphate aldolase | –1.42 | 8.85E-05 |
| AW132483 | FTSH-like protease | –1.05 | 1.45E-06 |
| AW831121 | Glutamate-1-semialdehyde 2,1-aminomutase | –1.68 | 8.12E-06 |
| AW508802 | Glyceraldehyde 3-phosphate dehydrogenase A | –1.63 | 8.4E-09 |
| AW132322 | HY5 (bZIP protein) | –1.08 | 4.28E-07 |
| AW432225 | Indole-3-glycerol phosphate synthase | –1.59 | 4.03E-08 |
| AI855484 | Inner-envelope membrane protein, 37 kDa | –1.34 | 1.61E-07 |
| AI495256 | Ketol-acid reductoisomerase | –1.48 | 1.3E-06 |
| AI855740 | LIL3 (light-harvesting complex gene) | –2.25 | 6.29E-10 |
| AI960811 | Malate dehydrogenase (NADP+) | –1.01 | 7.05E-07 |
| AW508032 | mRNA binding protein | –0.98 | 5.31E-05 |
| AW202208 | NADPH-protochlorophyllide oxidoreductase | –2.39 | 1.57E-07 |
| AI960984 | Omega-3 fatty acid desaturase | –2.09 | 1.43E-07 |
| AI900927 | Oxoglutarate/malate translocator | –0.44 | 5.52E-06 |
| AI900647 | Oxygen evolving enhancer protein 1 | –1.84 | 2.19E-09 |
| AW156360 | Oxygen-evolving enhancer protein 2 | –1.73 | 3.1E-08 |
| AW397159 | Oxygen-evolving enhancer protein 3 | –1.28 | 9.44E-07 |
| AW508183 | Phosphoglycerate kinase | –1.45 | 1.94E-07 |
| AI965987 | Phospholipid hydroperoxide glutathione peroxidase | –0.85 | 1.13E-08 |
| AI461189 | Phosphoribulokinase | –2.60 | 1.03E-09 |
| AW132544 | Photosystem I protein psaH | –1.86 | 1.69E-08 |
| AI460480 | Photosystem I reaction center subunit II | –1.08 | 1.78E-06 |
| AW508794 | Photosystem I reaction center subunit III | –1.14 | 4.22E-09 |

(*Continued on next page*)

[a] Log2 transformed fold change.
[b] *P* value from R/MAANOVA (Kerr et al. 2000; Wu et al. 2003).

or repressed in the same direction, but the HR-associated R response was quantitatively stronger in most cases. We noticed a similar trend in soybean occurring during Phases II and III of the interactions, which was visualized by plotting the differentially expressed genes of the 8 hpi R response and, keeping the genes in the same order along the *x* axis, plotting differential expression for S at 8 hpi, S at 24 hpi, and R at 24 hpi (Fig. 4). The trend plot indicated that the genomic response to S and R interactions in soybean, as in *A. thaliana*, followed a similar trend. In general, genes that increased or decreased in abundance in the R response tended to be similarly represented in S response. Although the direction of differential expression tended to be similar with a coefficient of determination ($r^2$) between samples of at least 0.76, the degree of differential expression for many genes differed significantly between the R and S interactions, with the genes at 8 hpi showing a greater degree of differential expression than at other timepoints. The degree of expression level change was R 8 hpi > R 24 hpi > S 24 hpi > S 8 hpi.

Although the general trend of expression of this 8 hpi gene set was the same, many individual genes had a statistically significantly different response when comparing treatments at a *P* value cutoff of 0.0001. Statistical analysis allowed for the identification of gene transcripts that were significantly altered during both the R and S interactions compared with the $MgCl_2$ control. The Phase II 8 hpi analysis identified 398 gene transcripts as being commonly altered in both R and S responses in comparison to the $MgCl_2$ control, 310 genes being activated and 88 suppressed. We divided these 398 genes into two groups. The first group consisted of 124 genes, in which the difference in transcript level between R and S was not significant (Fig. 3B). The second group consisted of 274 genes showed a significant difference in transcript level between the R and S responses (Fig. 3C). The categories (ignoring miscel-

**Table 1.** (*Continued from previous page*)

| GenBank ID | Annotation | Fold change | *P* value |
|---|---|---|---|
| Down-regulated in R at T8 (*continued*) | | | |
| AW119594 | Photosystem I reaction center subunit IV | –2.30 | 3.29E-09 |
| AW277960 | Photosystem I reaction center subunit psaK | –1.54 | 1.98E-07 |
| AW309010 | Photosystem I reaction center subunit V | –1.92 | 7.2E-09 |
| AI495711 | Photosystem I subunit XI | –1.64 | 5.56E-08 |
| AI901236 | Photosystem II | –2.16 | 2.38E-09 |
| AI900654 | Photosystem II 22-kDa protein | –1.70 | 4.68E-08 |
| AW432399 | Photosystem II core complex proteins psbY | –2.11 | 1.63E-06 |
| AI900720 | Photosystem II protein family | –1.80 | 2.62E-08 |
| AW317705 | Photosystem II protein X | –1.95 | 7.82E-09 |
| AI736976 | Photosystem II reaction center | –1.72 | 1.42E-09 |
| AW317689 | Photosystem II stability/assembly factor HCF136 | –1.40 | 9.09E-05 |
| AW185639 | Plastocyanin A | –2.41 | 7.29E-07 |
| AW780591 | Plastocyanin B | –2.30 | 3.92E-07 |
| BE020281 | PPF-1 (GA inducible, Ca import in chloroplast) | –0.98 | 8.98E-08 |
| AW099417 | Proteasome regulatory particle | –1.15 | 1.85E-06 |
| AI460668 | Protein At2g37660, chloroplast precursor | –1.21 | 3.8E-08 |
| AW704061 | Protochlorophyllide reductase | –3.43 | 6.2E-12 |
| AI437758 | Ribonucleoprotein | –1.79 | 1.77E-08 |
| AI507827 | Ribonucleoprotein A | –2.27 | 5.88E-12 |
| AW101250 | Ribosome (30S ribosomal protein S1, CS1) | –2.03 | 5.03E-09 |
| AW397353 | Ribosome (50S ribosomal protein CL25) | –1.25 | 4.14E-05 |
| BE022188 | Ribosome (50S ribosomal protein L15, CL15) | –0.78 | 9.55E-05 |
| AI440864 | Ribosome (50S ribosomal protein L21) | –1.57 | 8.07E-09 |
| AI748521 | Ribosome (50S ribosomal protein L28) | –0.87 | 7.24E-05 |
| AW509218 | Ribosome (50S ribosomal protein L34) | –1.44 | 1.51E-07 |
| AW099544 | Ribosome (ribosomal protein L35) | –0.84 | 5.64E-05 |
| AW133362 | Ribulose-phosphate 3-epimerase | –0.63 | 7.51E-07 |
| AW507594 | RNA-binding protein RNP1 | –1.30 | 2.01E-06 |
| AI441594 | RuBisCO | –2.17 | 3.59E-08 |
| AI900697 | Sedoheptulose-bisphosphatase | –1.82 | 1.07E-08 |
| BE020505 | Stromatin | –1.92 | 9.34E-13 |
| BE020523 | TatC (pH-dependent protein transporter) | –0.61 | 9.23E-07 |
| AI939035 | Thiamin biosynthesis protein THI1-1 | –1.07 | 6.66E-07 |
| AW278662 | Thioredoxin (M-type 4) | –0.77 | 2.01E-07 |
| AW133478 | Thioredoxin reductase | –0.70 | 5.17E-05 |
| AI901185 | Thylakoid lumen 18.3-kDa protein | –1.87 | 3.38E-08 |
| AW185858 | Thylakoid lumenal 17.4-kD protein | –0.82 | 8.51E-05 |
| AI900944 | Thylakoid lumenal 17.9-kDa protein | –1.04 | 3.07E-07 |
| AW760677 | Thylakoid lumenal 25.6-kDa protein | –1.60 | 2.69E-05 |
| AW201992 | Translation elongation factor G (EF-G) | –1.46 | 5.33E-05 |
| AW202295 | Translation elongation factor Tu (EF-Tu) | –1.36 | 8.02E-06 |
| BF070743 | Translation initiation factor 2 (IF-2) | –1.66 | 1.71E-06 |
| AW459300 | Triose phosphate/phosphate translocator | –1.41 | 2.61E-07 |
| AW507890 | Triose-phosphate isomerase | –0.72 | 2.17E-05 |
| Up-regulated in R at T8 | | | |
| AI460836 | Catechol oxidase | 3.06 | 7.54E-12 |
| AW102121 | Glucose-6-phosphate isomerase | 1.12 | 5.15E-07 |
| AW102262 | Glutamate synthase | 1.60 | 6.01E-08 |
| AW100946 | Glycerol-3-phosphate *O*-acyltransferase | 1.27 | 5.66E-07 |
| AI441654 | Photoreceptor-interacting protein | 0.56 | 6.97E-05 |
| BE021537 | Tic40 | 0.55 | 2.34E-07 |
| AW471655 | Triose phosphate/phosphate translocator | 0.91 | 3.05E-07 |

laneous, no hits, and unknown) with the highest number of significantly differentially expressed genes were defense, heat shock, secondary metabolism, and signaling (Fig. 3C). All or most of the gene transcripts in the above categories were increased in abundance. For example, genes showing homology to heat-shock proteins HSP 60, 70, 80, 91, and DNAK were all increased in abundance. Many genes homologous to defense-related genes were also increased, but two such genes, a homolog of PAR-1b (AW307505) and an *MLO*-like gene (BE020055) decreased. As an indicator of responses to changes in oxidization levels, several genes in the oxidation category (e.g., *GST*, *AOX*, peroxidase) increased; however, most of the lipoxygenase homologs decreased.

In Phase III, sampling at the 24 hpi timepoint revealed a common set of 615 gene transcripts that were elevated and 294 reduced in abundance in both R and S, as compared with the $MgCl_2$ infiltration control. As an indication that both R and S plants were undergoing a high degree of stress during Phase III, many homologs of secondary metabolism genes were increased in transcript abundance in both T24 groups (Fig. 3D and E). Transcripts of protein synthesis–related genes, such as ribosomal subunits, were also increased in common responses of R and S (no significant difference between R and S). Ten LRR-type *R* gene homologs (AW432320, AI496325, AI496590, AW423328, AW509337, AW185705, BE020602, AW203459, AW423913, and AI461033) increased in both treatments and two LRR-type homologs (AW307311, AW100734) were significantly decreased in abundance in both R and S at 24 hpi. Two of these LRR-type homologs (AW203459, AW423913) were significantly higher in R than S at 24 hpi, whereas two (AI461033, AW100734) were significantly higher in abundance in S than R at 24 hpi.

On the trend plot (Fig. 4) one can notice a peak during Phase III in the 24 hpi R response (T24-R) that deviated from the trend. This peak also was weakly apparent in S at 24 hpi. Unlike the other genes on this trend plot whose differential expression in T8-R was higher than T24-R in this region, 304 genes showed higher transcript abundance in T24-R than in T8-R samples. About one third (106 out of 304) of these genes were annotated as being related to ribosomes.

**Phase II and III: S-specific expression.**

Of the 3,897 differentially expressed genes across the study, only 45 were specific to the S response. The major categories of these 45 genes were, listed in order of frequency, signaling, unknown, no hits, defense, and miscellaneous (Fig. 3F). Although these genes were S specific during Phase III in the T24 samples, none were also S specific in the Phase II T8 samples, and therefore, no gene was identified as being S specific across all timepoints. Virtually all of these S-specific genes (44 out of 45) increased in transcript abundance in S when compared with the $MgCl_2$ control. Some examples of genes in this group were *R* gene homologs (AI973594, AW234414, and AW756306), G-protein related (BE021450, AW307062 and AW306804), and protein kinase homologs (AW306978, AW706972, AI900656, AI437496, and AI855716).

**Phase II and III: R-specific expression.**

Differential gene expression between R and S was striking in Phase II and III. Approximately one tenth (2,229) of the 27,684 genes screened were differentially expressed between R and S at 8 hpi, based on transcript levels, and one twentieth (1,216) of the genes at 24 hpi. These genes included some involved in many plant processes previously shown to respond to biotic and abiotic stresses, such as genes involved in modifying cell walls, membranes, proteins, nucleic acids, cytoskeleton, signaling, primary and secondary metabolism, energy, and oxidation states (Fig. 3G and H).

A

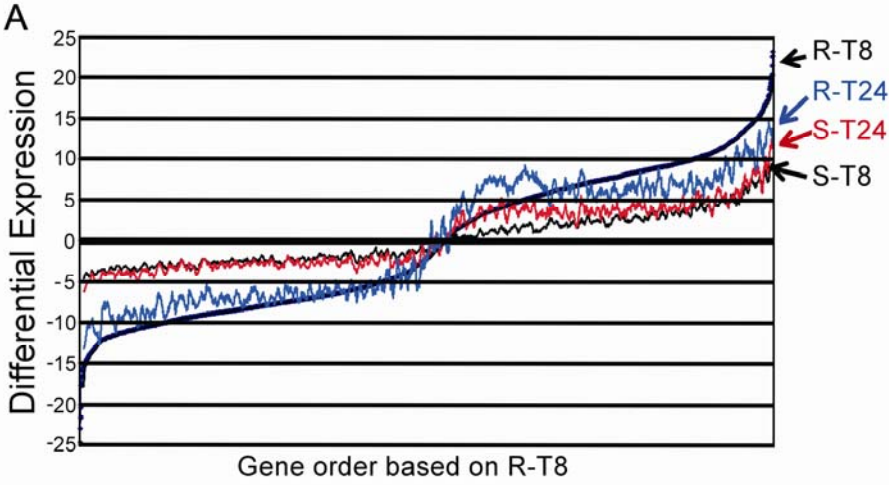


B

| | R-T8 | S-T8 | R-T24 | S-T24 |
|---|---|---|---|---|
| R-T8 | 1 | | | |
| S-T8 | 0.88 | 1 | | |
| R-T24 | 0.86 | 0.76 | 1 | |
| S-T24 | 0.82 | 0.85 | 0.83 | 1 |

**Fig. 4. A,** Trend plots revealing quantitative nature of soybean response during hypersensitive response–associated resistance (R) and susceptible (S) interactions. The relative gene expression of 3,897 genes expressed as *t* value (fold change divided by standard error) of expression differences comparing R with $MgCl_2$ at T8 (R-T8), R to $MgCl_2$ at T24 (R-T24), S to $MgCl_2$ at T8 (S-T8), and S to $MgCl_2$ at T24 (S-T24). Gene order along the *x* axis was determined by expression level at R-T8 samples. Other plots were drawn keeping the gene order the same as in R-T8. **B,** Table of pair-wise correlations among the samples.

Several other functional classes were also strongly associated with downregulation in the incompatible R interaction. A total of 17 of the 19 lipoxygenase genes (28 spots falling into eight different The Institute of Genomic Research (TIGR) tentative consensuses (TC) and 11 singletons) that showed differential transcript levels during the entire experiment were reduced in abundance. The only lipoxygenase transcripts that had an increased abundance were AI938417 and AW832618. Aquaporin transcripts were mostly reduced in R, with 24 of 32 specifically decreased in abundance during Phase II. Only one putative aquaporin (AW472220) showed a significant increase in RNA abundance in both R Phase II and III samples. Disturbance of the cytoskeleton during Phases II and III was apparent, as 51 of the 56 differentially expressed genes annotated as being related to actin, tubulin, and other cytoskeleton components decreased in abundance during the experiment, with seven (AI441284, AI901241, AI443426, AW832640, AI443445, AW666395, and AW394446) and 26 being R specific at both 8 and 24 hpi, respectively. The only cytoskeletal gene homolog that was R specific and increased in abundance at 8 hpi was a putative tubulin folding cofactor B (AI443429), whereas a putative actin organization protein, Villin 2 (AW707001), and an actin depolymerizing factor (AW397117) specifically increased in the R response during both Phase II and III. Additional categories that were

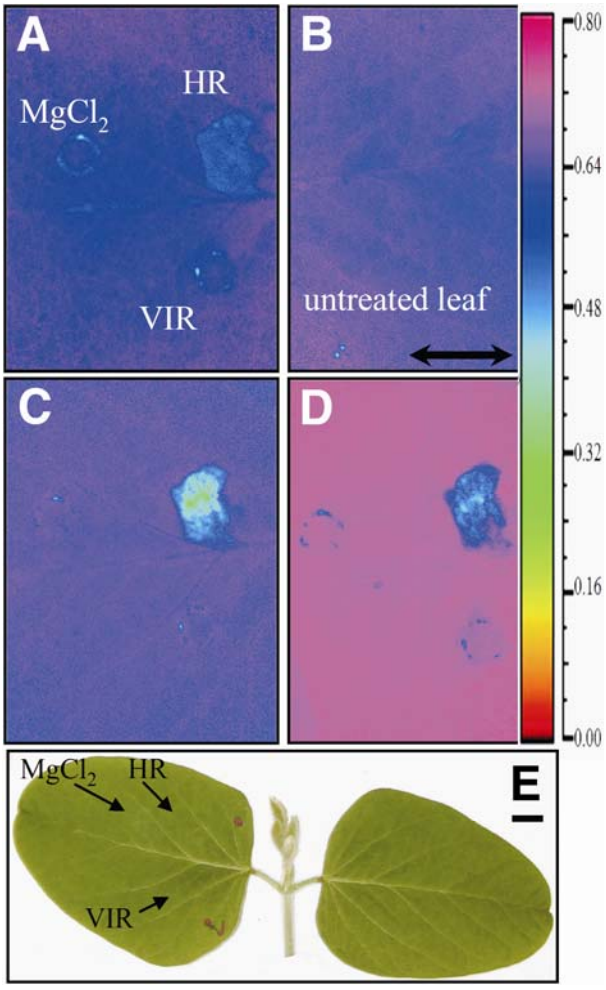


**Fig. 5.** False-color images of photosystem II operating efficiency of inoculated and uninoculated leaflets and dark-adapted $F_v/F_m$ of the same inoculated leaflet. R = infiltration with *Pseudomonas syringae* pv. *glycinea* provoking hypersensitive response–associated resistance, suspended in 10 mM $MgCl_2$. S = infiltration with *P. syringae* pv. *glycinea* provoking susceptible interaction, suspended in 10 mM $MgCl_2$. $MgCl_2$ = infiltrated with 10 mM $MgCl_2$ **A,** The area R showed significant depression (approximately 13%) of photosynthetic efficiency at 8 h postinoculation (hpi) in this false-color image of photosynthetic efficiency. **B,** False-color image of the $\Phi_{PSII}$ of an uninoculated, control leaflet at 8 hpi. **C,** False-color image of the $\Phi_{PSII}$ of the same infiltrated leaflet as in panel A, at 24 hpi. In area R, $\Phi_{PSII}$ was depressed by 41%. **D,** False-color image of the dark-adapted $F_v/F_m$ of same leaf infiltrated in panels A and C, at 24 hpi. Area R had 31% lower maximum operating efficiency than the rest of the leaflet. **E,** The reflected image of the same plant illustrates that there was no visible necrosis associated with any of the treatments at 8 hpi. As a consequence, the depressed $\Phi_{PSII}$ can be directly linked to the impairment of photosynthetic electron transport. Areas S and $MgCl_2$ did not show depressions of $\Phi_{PSII}$ outside the physical damage caused by the inoculation procedure (light blue circles noticeable in A and D. Scale bars represent 1 cm. The bar in panel B and the false-color scale (right) are applicable to all fluorescence images.

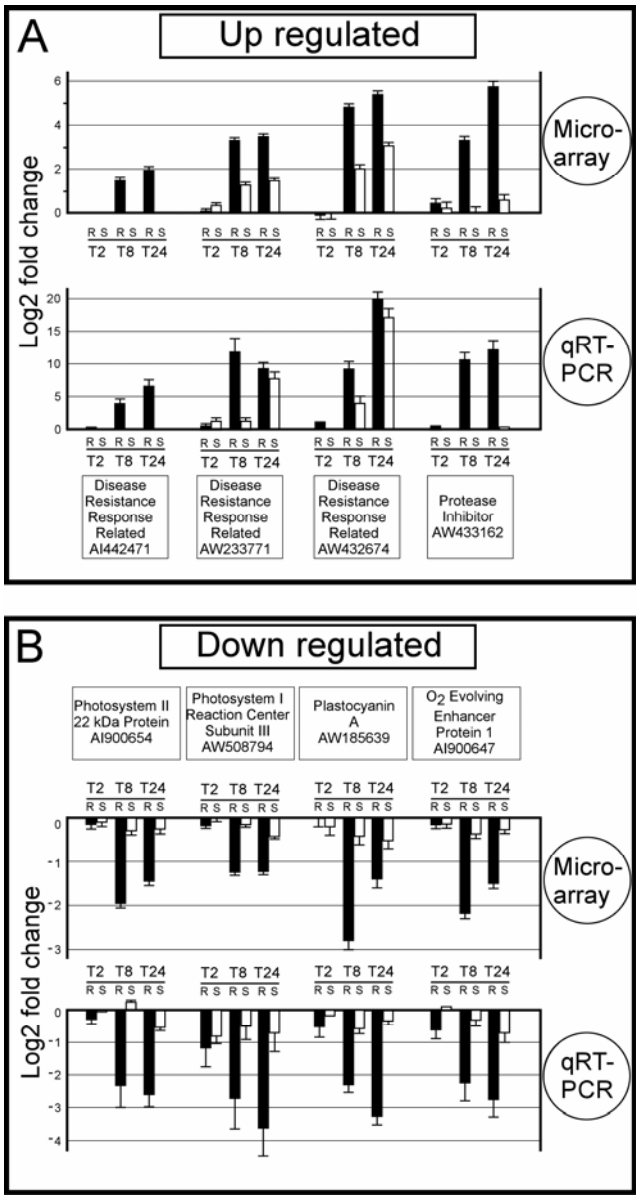


**Fig. 6.** Microarray verification using quantitative real-time reverse-transcription-polymerase chain reaction (QRT-PCR). Expression levels of selected genes that showed **A,** increased or **B,** decreased, respectively, levels of RNA abundance were reevaluated by QRT-PCR. Expression level change is given as log2-transformed fold change of resistant (R) or susceptible (S) treatments compared with the $MgCl_2$. Black bars represent R treatment and white bars represent S treatment. QRT-PCR data represents the mean value obtained from three independent amplifications, and the error bars indicate the standard error of the mean. Error bars of microarray data provided by MAANOVA (Kerr et al. 2000; Wu et al. 2003). Note that different scales are used in the graphs.

largely decreased specifically during the R response included genes annotated as pectin-related, proline-rich proteins, hormone-related except jasmonic acid–related (ABA and ethylene up and down), and genes specific to the anthocyanin branch of the phenylpropanoid pathway. We observed a possible interaction between the defense response and the gibberellic acid (GA) signaling pathway, as gene transcripts that are responsive to GA, such as *GAI1* and *GIP1* homologs, were decreased in abundance.

Differential levels of gene transcripts specific to R in Phase II and III included a large number of genes (over 100 genes in each group) involved in primary metabolism, membrane transport, gene regulation and signal transduction, and defense. In particular, we observed a striking pattern for genes involved in photosynthesis. Of the 27,684 genes represented on the microarrays, there were a total of 452 clones (equivalent to 296 TC or singletons) with an annotation related to chloroplast or photosynthesis, and 202 of these showed measurable differential expression. A total of 92% (186 of 202) of these chloroplast-related genes were significantly reduced in transcript abundance during the R response. Focusing on the 8 hpi timepoint and removing the possible redundancies based on common TC numbers and common annotation produced a list of 94 decreased and 7 increased chloroplast-related gene transcripts showing significantly different abundance in R (Table 1). One aberration was a putative nitrite transporter (AI437942) that was specifically reduced in abundance for incompatible Phase II samples but significantly higher in abundance in Phase III at 24 hpi compared with the S Phase III sample. In addition, only one gene annotated as being chloroplast-related, a putative ferrochelatase (AI938531), was significantly up in both R and S.

**Miscellaneous observations of differential gene expression.**

As an indication of a response to oxidative stress, all 24 GST out of the set of 3,897 differentially expressed genes were more abundant during the R response. Cellular proteins were also apparently undergoing significant modification and trafficking as indicated by the strong increase of gene transcripts similar to heat-shock proteins, proteases, and protein folding and prenylation enzymes. Heat-shock protein transcripts were largely increased in both R and S responses, but 18 increased and 8 decreased in the R response. A total of 100 proteolysis-associated gene transcripts were differentially expressed during the experiment, with 65 being up in their abundance compared with the control. Many of these proteolysis genes were apparently R specific, as 41 were specifically increased in R and 28 were specifically decreased in R. Three EST (AW099579, AW459597, and AW432994) that represented protein disulfide isomerase protein refolding enzymes were R-specifically increased in Phase II but not in Phase III, as their level in the S sample was also significantly increased in Phase III T24 samples compared with the control. A total of 60 EST with similarity to calcium signaling genes were significantly differentially expressed during the experiment. Of these 60, 11 transcripts were specifically down in the R and 20 were specifically up in abundance. The increased calcium signaling-related transcripts included four (AI460551, AW278834, AI437703, and AW433261) that had high homology to calmodulin and were also significantly increased in the T2 $MgCl_2$ versus the T2 untouched control.

**Physiological measurements support downregulation of photosynthetic activity.**

Chlorophyll fluorescence measurements revealed localized depressions (approximately 10%) in PSII operating efficiency ($\Phi_{PSII}$) in areas inoculated with the R-inducing strain of *P. syringae* pv. *glycinea*, apparent in Phase II by 8 hpi (Fig. 5). Since there were no visible symptoms of damage at this stage, the decrease in $\Phi_{PSII}$ was not associated with a change in leaf spectral properties and can be directly linked to a depression in photosynthetic electron transport. This decrease also correlated with an approximately 20% depression of the dark-adapted fluorescence parameter $F_v/F_m$ (maximum quantum efficiency of PSII), interpreted under the conditions of the experiment, as direct damage to PSII reaction centers. After 8 hpi, the $\Phi_{PSII}$ and $F_v/F_m$ of areas infiltrated by the avirulence strain of *P. syringae* pv. *glycinea* continued to decrease, having values four times lower at 24 hpi (Fig. 5). The virulent strain and $MgCl_2$ infiltration did not affect any of the chlorophyll fluorescence parameters outside the areas mechanically damaged by the infiltration procedure.

**Verification of array data with quantitative real-time polymerase chain reaction.**

As a means to validate the microarray results, 10 gene transcripts that were found to change in our microarray study were further analyzed with quantitative real-time polymerase chain reaction of reverse transcribed RNA (QRT-PCR) on an entirely new set of biological samples. The QRT-PCR results for a subset of genes indicated similar trends of changes in mRNA abundance consistent with the microarray results, supporting that the arrays accurately identified genes induced or repressed due to inoculation (Fig. 6). Within the set of verified genes, two induced within 24 h of inoculation with the R-inducing pathogen, a disease-resistance response-related gene (AI442071) and a protease inhibitor gene (AW433162). These two genes might represent good candidates as markers for HR-associated resistance in soybean, as both were highly up-regulated in the R response during Phase II and III, with virtually no change in the S response at these timepoints. The magnitude of change in expression level following the treatments typically was greater when determined by QRT-PCR than from the microarray experiment.

## DISCUSSION

The response of soybean to inoculation with compatible and incompatible *P. syringae* pv. *glycinea* leading to susceptible or HR-associated resistance was analyzed using cDNA microarrays. By minimizing non–treatment related variation, utilizing an experimental design involving multiple technical and biological replicates and by analyzing the data by analysis of variance (ANOVA), we were able to provide strong statistical support (FDR < 1) that 3,897 genes responded during the course of the experiment. The complete experiment has been deposited in the NCBI Gene Expression Omnibus (GEO) database as accession number GSE2961.

**Identifying significant gene-expression changes associated with Phase I, the induction stage for plant defense responses at 2 hpi.**

Although differential gene expression was not as striking at 2 hpi as at other timepoints, there was a statistically significant change in the expression levels of 172 genes compared with the T2 null control, which was presumably in response to the physical treatment of the plants during inoculation and immediate stress signaling. A total of 77% (133 of 172) of the gene transcripts that were increased in T2 vacuum-infiltrated samples were also increased specifically in either the T8, T24, or both samples from either R or S interactions compared with the $MgCl_2$ T8 and T24 samples, indicating that many of these genes are apparently important players in defense to pathogens in addition to being early general stress-response genes. Many of these genes had annotations supporting a possible role in regula-

tion of cellular physiology (i.e., transcription factors, LRR homologs, calmodulins), and our results are in agreement with other plant-pathogen studies of initial response to pathogen or stress, as detailed in several reviews (Lamb and Dixon 1997; Mahalingam and Fedoroff 2003; Scheel 1998; Wan et al. 2002).

To identify genes that might be specifically affected by the bacterial pathogens during Phase I, it was necessary to utilize a less stringent *P* value reflective of the biology, as presumably few cells and few transcripts would be responding by 2 hpi compared with the other timepoints. Lowering the stringency of selection in this manner revealed the possible involvement of heat-shock proteins as an important early response in soybean to pathogen infections. In addition, several *GST* genes showed greater abundance in S treatment than in R treatment, which suggests a possible role in maintaining a lower oxidative state of the host in S than in R responsive tissue. As suggested by Foyer and Noctor (2003, 2005), balancing ROS and antioxidants is at the heart of fine control of environmentally induced conditions and could be a critical factor in determining the outcome of plant pathogen interactions.

**During the effector or amplification Phase II (8 hpi), clear expression differences were observed between R and S.**

In this current study, we identified differential levels of soybean homologs of several key genes, such as *EDS1*, *NDR1*, *LSD1*, and *DAD1*, all of which could be considered as modulators of the Stage II amplification phase. In *A. thaliana*, mutation of these genes leads to inability to effectively regulate PCD. Jabs (1999) suggested that such factors could serve as self-amplifying rheostats that sense and respond to a variety of signals, such as redox, SA, or ROS, to control PCD. Zhang and associates (2004) identified at least three feedback loops, involving NDR1, NPR1, and salicylic acid, in *A. thaliana* that control progression of HR-associated resistance induced by *P. syringae*.

ROS is a major signal leading to PCD. When plants are inoculated with an incompatible HR-inducing pathogen, a second, much more intense, burst of ROS is measurable, marking the transition from Phase I into Phase II (Doke 1983; Lamb and Dixon 1997). This Phase II oxidative burst is generally lacking in compatible susceptible interactions. Levels of ROS can be influenced by various oxidative enzymes, such as NADPH oxidases, catalases, and peroxidases, found in several locations throughout a cell (Mahalingam and Fedoroff 2003). The importance of these enzymes in defense was demonstrated by effects of exogenous $H_2O_2$ leading directly to PCD (Levine et al. 1994) and $H_2O_2$ produced in a catalase-deficient tobacco transgenic (Vandenabeele et al. 2003) as well as by antisense cytosolic ascorbate peroxidase transgenics that showed spontaneous cell death (Takahashi et al. 1997), implying the inability to control amplification of PCD signaling. Smirnoff and Wheeler (2000) state that ascorbate peroxidase is emerging as the key enzyme in fine control of $H_2O_2$ concentrations in plants. In our study, a range of expression patterns from oxidative enzymes suggest that their role in regulating ROS is complex.

The photosystem centers of chloroplasts are another potential source of ROS, and experimental evidence is mounting that PSII may be a major source of the large secondary oxidative burst specific to HR-associated resistance. The D1 subunit of PSII has evolved to be a labile protein, and its destruction leads to photooxidation of molecules in and around PSII, including formation of singlet oxygen and hydrogen peroxide (Barber and Andersson 1992; Foyer and Noctor 2003; Laloi et al. 2004). It may seem paradoxical that D1 would be easily damaged as this leads to photoinhibition in strong sunlight (Barber and Andersson 1992). However, it may be advantageous if plant cells could regulate the destruction and repair of D1, so as to tap the energy of the sun to rapidly generate high ROS levels during pathogen attack, therefore destroying the pathogen and defending against disease. D1 removal and replacement has been shown to be regulated in a complicated manner involving at least two proteolytic steps, the first involving an unknown GTP-dependent process and the second involving FTSH, an ATP-dependent protease (Spetea et al. 1999). Reduction in levels of *FTSH* transcription was associated with HR in tobacco (Seo et al. 2000) as well as in *Nicotiana benthamiana* (Matsumura et al. 2003). We also observed a reduced abundance of *FTSH* homologs (AW132483 and AW156684) during the HR-associated R response in our study. What triggers the initial damage and proteolysis of D1 during pathogen attack and how plant cells regulate the consequence of D1 destruction remains unknown. Does rapid D1 degradation during HR lead irreversibly to PCD, or can cells regulate the progression of D1 degradation and advancement of the HR, so as to generate an environment that is temporarily lethal to the pathogen without necessarily provoking death of the plant cell? That some plant-pathogen interactions can lead to gene-for-gene specific HR-associated resistance without cell death (Bendahmane et al. 1999; Clough et al. 2000) suggests that the intensity of the HR can be regulated. In addition to leading to pathogen damage, damaged PSII would also lead to reduction in sugar production, thereby limiting the amount of energy available to support rapid growth of a pathogenic microbial population. Likewise, the reduced production of aquaporins as noted in Phases II and III could reduce photosynthesis (Aharon et al. 2003; Lawlor 2002) as well as prevent bacterial multiplication by keeping water from the apoplast (Wright and Beattie 2004).

Interestingly, pathogens seem to have evolved to tap into the ability of a potential host to initiate a defense reaction, for it has been shown that, if the HR is successfully blocked, a pathogen may lose its ability to provoke disease and colonize the tissue. For example, transgenic tomato plants expressing the p35 protein (a protease-inhibitor that blocks apoptosis in insects) were defective in HR but also had increased resistance to a broad range of tomato pathogens, suggesting that successful parasitism depended upon achieving the partial activation of the plant PCD system (Lincoln et al. 2002). It would be interesting to know if p35 affects the proteases that degrade D1.

The possible strategy of tapping into the light-harvesting energy of the chloroplasts to generate ROS for defense was first proposed by Allen and associates (1999). *Asparagus sprengeri* suspension cells were used to produce evidence that chloroplast electron transfer is disrupted during HR-associated resistance and that the photosystems may be generating a light-inducible HR-specific ROS, presumably the result of PSII still being oxidized in the light during the oxidative burst (Allen et al. 1999).

As in the study of Allen and associates (1999), we also observed a reduction in photosynthesis following inoculation with the pathogen. We observed 94 of 101 differentially expressed chloroplast-related genes being down in abundance, likely coordinately regulated in response to changes in the redox state of the cell (Pfannschmidt 2003). In addition, physical measurements of the spatial pattern of chlorophyll fluorescence on attached soybean leaves indicated that depressions of $\Phi_{PSII}$ during Phase II at 8 hpi in leaf areas infiltrated with the HR-inducing strain of *P. syringae* pv. *glycinea* were caused by direct damage to PSII reaction centers (Fig. 5). This damage could occur by D1 degradation, as discussed above, in addition to the direct action of HR-induced ROS on the photosynthetic machinery or as a consequence of localized apoptosis and associated changes in the pigment matrix.

The similarity of our transcript profiling data to changes in expression levels observed in CAT1AS, a catalase-deficient to-

bacco transgenic (Vandenabeele et al. 2003), provides additional support for the role of ROS in signal transduction leading to HR-associated resistance in soybean. When CAT1AS plants were induced by light stress to generate high levels of $H_2O_2$, transcripts induced included those predicted to be heat-shock protein, transcription factors, proteases, transporters, hormone synthesizers, and many others that are homologous to those observed to be expressed in an R-specific manner in our study.

Although we noted decreased abundance of nearly 100 chloroplast-related genes, we also noted activation of seven chloroplast-related genes in response to R. These up-regulated genes (such as AI441654, a putative photoreceptor-interacting protein) are candidates for being possible players in the activation of photoinhibition during HR-associated resistance. One such gene that just missed the $P \leq 0.0001$ cutoff to make the list (Table 1) of chloroplast-related genes that were differentially expressed at 8 hpi was AI901230, an *LLS1*/*ACD1* homolog. Mutations in *LLS1* or *ACD1* caused plants to lose their ability to restrict lesion spread (Gray et al. 1997; Greenberg and Ausubel 1993). Interestingly, this *LLS1*/*ACD1* homolog was slightly down-regulated in S at 8 hpi (log2 ratio of –0.45, $P = 0.0028$) and slightly up in R at 8 hpi (log2 ratio of 0.53, $P = 0.000116$), further supporting its possible importance in defense. LLS1/ACD1 has been identified as a pheophorbide a oxygenase, which is a Rieske-type iron-sulfur cluster-containing enzyme that regulates chlorophyll catabolism, specifically the degradation of pheophorbide (Pruzinska et al. 2003). That *lls1* and *acd1* mutants fail to limit lesions suggests that chlorophyll breakdown is required for mediation of the HR (Gray et al. 1997; Greenberg and Ausubel 1993).

**Phase III: Cell destruction and repair.**

In Phase III, plant cells of resistant tissue are either undergoing PCD, actively protecting themselves from PCD, or both. Many genes reported to be related to plant PCD were observed to be differentially expressed in our study. However, many of these PCD-related genes were not completely R specific but were also similarly induced or repressed in the compatible S interaction in either Phase II, Phase III, or both. Genes specifically induced during Phase III HR-associated R and annotated as PCD-related included: AW508851 (HR inducer), AW395910 (HR inducer), AI440598 (*PCAR*, apoptosis-related protein in human), AW432916 (*NDR1*/*HIN1*-like), AI440724 (*NDR1*/*HIN1*-like), and AI901230 (*LLS1*/*ACD1*-like protein). The only HR-specific, down-regulated genes were AW424240 (Avr induced), BE020921 (harpin induced), AI900637 (*NDR1*/*HIN1*-like), and AI442370 (*TED4*, apoptosis inhibitor). That two *NDR1*/*HIN1* homologs had opposite expression patterns is probably a reflection of incomplete sequence information, as the two EST fit into two different TC, and AI900637 is 87.8% similar to *NDR1*/*HIN1* over 78% of its sequence, while AI440724 is 82% similar over just 43% of its sequence, suggesting the possibility that these are two different but closely related genes.

Oxidative signaling and damage leads to necrosis. If oxidizing free radicals can be scavenged by antioxidants, necrosis and host-cell damage can be minimized. For example, ROS scavengers allowed *P. syringae* to multiply to higher numbers in tobacco (Keppler and Baker 1989). Overexpressing ferritin, a protein that sequesters iron, which is the major generator of the hydroxyl radical (OH•), prevented stress-induced necrosis, including that induced by necrotrophic plant pathogens (Deák et al. 1999). Therefore ROS scavengers may benefit both host and pathogen. A major class of antioxidants in soybean is the isoflavones, which benefit soybean by being both antioxidative and antimicrobial. Lamb and Dixon (1997) suggest that the isoflavonoid phytoalexin pathway might have evolved for oxidative defense and, therefore, may be major players in regulating the degree of oxidative signaling and cellular damage. A strong induction of the flavone and isoflavone branches of the phenylpropanoid pathway (Winkel-Shirley 2001) was observed in both Phase II and Phase III samples.

Oddly, lipoxygenases were largely down-regulated in our study, while many other reports have stated that lipoxygenases are often stress- and pathogen-induced (Keppler and Novacky 1987; Koch et al. 1992; Rusterucci et al. 1999). Our data, supported by Moy and associates (2004), who also noted a consistent reduction in lipoxygenase mRNA abundance in soybean infected with a virulent strain of *Phytophthora sojae* compared with a healthy control, suggests that lipoxygenases might respond differently in soybean than in some other plants in response to pathogen.

Cells were actively responding to protein and cellular damage in our study, as noted by the increase in ribosomal gene expression during Phase III for the R samples. It is uncertain if this apparent increased protein synthesis is generated from individual cells triggered for R or from neighboring cells that are not undergoing PCD. This increase in protein synthesis might also be indicative of the need to redirect cellular resources.

**Summary.**

The presented expression study identified nearly 4,000 genes that were differentially expressed due to pathogen inoculation and provides a large pool of genetic material for further in-depth analyses of the role of specific genes in pathogen defense. For example, many of the differentially expressed genes had homology to regulatory and signal transduction–related genes and over 1,000 genes were of unknown function. Our study also further supports the developing theory that chloroplasts may be key players in plant defense, as the loss of integrity of PSII, specifically subunit D1, may be the source of the HR-associated oxidative burst and would also lead to limited amounts of available simple sugars, thereby restricting pathogen growth. Discovering how plants regulate the destruction and repair of PSII during defense promises to be fascinating and may generate strategic targets for genetic enhancement of disease resistance.

## MATERIALS AND METHODS

To enhance our ability to identify the genes that were differentially expressed in response to inoculation, several steps were taken to minimize the biological variation not related to our specific treatments. One step was to use a soybean cultivar that has gone through years of selfing, resulting in highly homozygous individuals and providing low plant-to-plant genetic variation. Second, an environmental growth chamber was used to provide consistent, controlled conditions for each set of biological repeats. Third, the tissue assayed was from fully expanded primary leaves that should have been undergoing little new growth or development. Fourth, we pooled leaves from multiple plants as the source of RNA. Fifth, we employed a loop experimental design that included multiple technical replicates per treatment. Sixth, the entire experiment was repeated and all data from both biologically repeated experiments were processed together, resulting in an overall experimental false discovery rate that was less than one.

**Plant treatment and RNA isolation.**

Soybean (*Glycine max* [L.] Merrill cv. Williams 82, RPG1 dominant) plants were grown at constant 22°C in 16 h of daylight with approximate light intensity of 100 to 120 µmol photons $m^{-2}s^{-1}$. To enhance stomatal opening, the growth chamber was kept under high humidity by flooding the chamber floor with water the day prior to inoculation. Plants were inoculated approximately 14 days after planting, when the primary unifoli-

ate leaves were completely expanded and the first trifoliate leaves were beginning to emerge. Inoculations were performed about 3 to 5 h after the day cycle began by inverting the pot (wrapped with parafilm the day before to prevent soil from falling out) into a 500-ml beaker filled with inoculum and were closed within a vacuum chamber. Vacuum was drawn for about 90 s and then was released rapidly, forcing the inoculum in through the open stomata and throughout the apoplastic space. Poorly infiltrated leaves (less than about four-fifths infiltrated) were not collected for analysis. Immediately after infiltration, the parafilm was removed and plants were placed back in the growth chamber. Bacterial inocula consisted of the strain *P. syringae* pv. *glycinea* race 4, with or without the avirulence gene *avrB*, on plasmid pVB01 suspended in 10 mM $MgCl_2$ at a concentration of 0.02 $A_{600}$ (corresponding to approximately $2 \times 10^7$ CFU $ml^{-1}$). Control leaves were vacuum-infiltrated with 10 mM $MgCl_2$. At 2 hpi, we also harvested leaves from plants that were not infiltrated, as "untouched" control. To obtain sufficient material and to minimize leaf-to-leaf variation, unifoliate leaves from three to four plants (five to eight leaves) were pooled. Collected leaves were immediately frozen in liquid nitrogen and were stored at –80°C before RNA extraction. The entire experiment was repeated one month later.

Total RNA was isolated, following the manufacturer's protocols, from pulverized, frozen tissue using TRIzol reagent (Invitrogen, Carlsbad, CA, U.S.A.) and Phase Lock Gel-Heavy (Brinkmann Instruments, Inc., Westbury, NY, U.S.A.). Samples were checked with a BioAnalyzer 2100 (Agilent Technologies, Palo Alto, CA, U.S.A.) to verify that RNA had not degraded, and the concentration of RNA in each sample was determined with a NanoDrop ND-1000 spectrophotometer (NanoDrop Technologies, Wilmington, DE, U.S.A.).

**Construction of cDNA microarray.**

The complete description of array construction has been described elsewhere (Vodkin et al. 2004). In brief, EST from 25 libraries representing cloned cDNA from a variety of tissues such as embryo, seed coat, flower, pod, root, stress-treated seedlings, and pathogen-infected tissue, were contigged to identify unigene sets to constitute rerack libraries Gm-r1021, Gm-r1070, Gm-r1083, and Gm-r1088. PCR products of the cDNA inserts of these clones were spotted, to generate three slide sets of 9,216 genes (27,648 total) per slide. Photosynthetic tissue represented the source of 69.6% of all genes, with root tissue being the source of 30.1%. Approximately one-fifth (1,784) of the root-derived genes came from *Rhizobium*-inoculated tissue. Genes from hormone-treated tissue made up 7.46% of the array, whereas cold, salt, drought, and pathogen-stressed tissue represented the source of 4.7, 0.7, 2.3, and 3.5% of the genes, respectively. All cDNA clones are available to the public from either Biogenetic Services (Brookings, SD, U.S.A.) or the American Type Culture Collection (Manassas, WV, U.S.A.).

As the construction of these soybean microarrays was based on cDNA sequence information, it is possible that some genes are represented by multiple clones. Although much effort was taken to minimize duplication, the maximum level of such redundancy for these soybean arrays has been estimated to be approximately 20%, meaning that the total number of unique genes assayed by the three slide sets is no lower than 22,000 (Vodkin et al. 2004).

**Annotation and functional classification.**

Annotations were based primarily on TIGR annotation as of December 2003, and secondarily using BLAST-X against the NCBI nonredundant database (Shoemaker et al. 2002; Vodkin et al. 2004). To simplify discussion of the large dataset, gene annotations were used to classify each gene into one of 16 functional categories: cell wall/cell development, cytoskeleton, defense, DNA/RNA, energy, fatty acid, heat-shock, hormone, membrane, oxidation, primary metabolism, protein, secondary metabolism, senescence, signaling, and stress (Table 2). The miscellaneous category was used for genes that did not fit into any of the above categories, the unknown category was used for genes that matched only a hypothetical or uncharacterized gene, and the no hit category was used for genes without significant homologs in sequence databases. Classification calls for genes that could fit multiple categories were prioritized as follows: signaling > energy > enzymology/function > response to specific stimuli > defense. Defense was our lowest priority because this was a study of a plant's response to pathogens and, therefore, all genes differentially expressed could be considered as defense-related. Nearly three-fourths (72%) of the genes had annotations allowing classification, and the other 28% were classified as either unknown (18%) or no hits (10%).

**Preparation of fluorescently labeled probes.**

Fluorescently labeled cDNA probes were prepared by reverse transcription of total RNA in the presence of amino-allyl-dUTP (aa-dUTP; Sigma, St. Louis), followed by coupling either with Cy3 or Cy5 monofunctional dye (Amersham Pharmacia Biotech, Piscataway, NJ, U.S.A.). The reverse transcription reaction was performed using 30 to 40 µg of total RNA concentrated to an 11-µl volume in a vacuum centrifuge. A sample of 11 µl RNA and 2 µl oligo $d(T)_{25}$ (3 µg/µl) was mixed and heated at 70°C for 10 min and was immediately chilled on ice for 10 min. Following centrifugation for 30 s at 13,000 × *g*, 17 µl of reverse transcription master mix (0.5 mM each of dATP, dCTP, and dGTP; 0.3 mM dTTP; 0.2 mM aminoallyl-dUTP [all nucleotides from Sigma]; 10 mM dithiothreitol [DTT] [Invitrogen]; 400 units of Superscript III reverse transcriptase [Invitrogen]; and 1× RT reaction buffer [Invitrogen]) was added for a total volume of 30 µl. After a 3-h incubation at 50°C, RNA was hydrolyzed by addition of 10 µl 1 M NaOH and 10 µl 0.5 M EDTA (pH 8.0) and was incubated for 15 min at 65°C. Samples were neutralized with 10 µl 1 M HCl. Newly synthesized cDNA was purified using QiaQuick PCR purification columns (Qiagen, Valencia, CA, U.S.A.) with modified Tris-free buffers (100 ml of wash buffer: 0.5 ml of 1 M $KPO_4$ [pH 8.5], 15.25 ml of $H_2O$, 84.25 ml of ethanol; 10 ml of elution buffer: 0.04 ml of 1 M $KPO_4$ [pH 8.5], 9.96 ml of $H_2O$). Successful reverse transcription was verified by measuring light absorption at 260 nm on a NanoDrop ND-1000 spectrophotometer (NanoDrop Technologies) to determine that cDNA yield corresponded to about 2 to 4% total RNA. Samples were dried by centrifugation under vacuum, followed by suspension in 4.5 µl of 0.1 M carbonate buffer (1 M $NaHCO_3$ made fresh monthly and adjusted to pH 9.0 using concentrated HCl). An addition of 4.5 µl of Cy3 or Cy5 monofunctional dye (#PA23001 and #PA25001 [Amersham Pharmacia], each tube of dye suspended with 73 µl of anhydrous dimethyl sulfoxide [Aldrich, Milwaukee, WI, U.S.A.] pipetted in single-use aliquots and stored at –80°C) was added to each sample. Labeling reaction was incubated for 1 h at room temperature in the dark. Unincorporated dyes from Cy3 and Cy5 reactions were removed using QiaQuick PCR purification columns (Qiagen). The column eluates were combined and the fluorescent labeling was verified using the NanoDrop ND-1000 spectrophotometer (NanoDrop Technologies). Light absorption at 260, 550, and 650 nm was measured to determine the concentration of cDNA and incorporated Cy3 and Cy5, respectively.

**Hybridization, wash, and scan.**

To the purified labeled probe (concentrated to 34 µl), 2 µl Poly $d(A)_{50}$ (50 µg/µl) was added, and this solution was placed

into just-boiled (95 to 99°C) water for 3 min. After centrifugation at 13,000 × *g* for 1 min, 36 µl of 2× hybridization solution (50% formamide, 10× SSC [1× SSC is 0.15 M NaCl plus 0.015 M sodium citrate], 0.2% sodium dodecyl sulfate, preheated to 42°C) was added. The solution was then pipetted onto a slide containing the array under a glass coverslip (LifterSlip, Erie Scientific Co., Portsmouth, NH, U.S.A.) and was incubated in a sealed chamber within a 42°C water bath for 16 to 24 h, and then, was washed (Hegde et al. 2000) and scanned for fluorescence emission using a Perkin-Elmer (Foster City, CA, U.S.A.) ScanArray Express microarray scanner.

**Experimental design and data analysis.**

Images were analyzed with GenePix version 4.0 software (Axon Instruments, Union City, CA, U.S.A.) to generate fluorescent intensity and background values for each spot in both the Cy3 and Cy5 channels. TIF images and GenePix result data files were uploaded into GeneTraffic (Iobion, La Jolla, CA, U.S.A.) for quality-control analyses. A loop design (Fig. 2) was used, and microarray expression data from GenePix result files was analyzed using the R/MAANOVA statistical program (Kerr et al. 2000; Wu et al. 2003). Each experiment was replicated twice in three sets of slides, each representing a different set of 9,726 soybean expression sequence tags. This multiloop design permitted the effective estimation of timepoint and treatment effects represented in each sample while accounting for other sources of variation. The response variable studied was the log2 of the normalized, background subtracted fluorescence intensity. A global normalization (glowess) was applied to the intensity data. These observations were analyzed using a linear mixed effects model. The fixed effects terms included in the model were dye and sample (time-treatment combination). The model also included the random effect of array. The array and errors were assumed to be normally distributed. The overall experiment effect was computed for each gene spotted, and the *P* values were adjusted for multiple testing, using the false discovery rate criterion of Benjamini and Hochberg (1995). Only those genes with $P \leq 0.05/9{,}726$ or 0.000005 were considered for further study, as each print library of 9,726 spots was analyzed separately.

**QRT-PCR.**

Total RNA was purified as described above for microarray analysis but purification was followed by a DNA removal treatment using the Ambion DNA-free kit (Ambion, Inc., Austin, TX, U.S.A.) to remove traces of genomic DNA. Purified, DNA-free, total RNA (1 µg) was converted into first strand cDNA by reverse transcription. RNA was denatured at 65°C for 5 min, followed by quick chilling on ice in a 13-µl reaction containing 1 µg of oligo(dT) 25-mers and water. After the addition of 4 µl of 5× reaction buffer (Invitrogen), 2 µl of 0.1 M DTT and 1 µl of 10 mM dNTPs, the reaction was preheated to 42°C for 2 min before adding 1 µl (200 units) of Superscript II reverse transcriptase (Invitrogen), followed by incubation at 42°C for another 50 min. After terminating the reaction by heating at 70°C for 15 min, the final reaction mix was diluted in water to a volume of 200 µl. Controls (minus

**Table 2.** Functional categories used to classify differentially expressed genes

| Category | Selection criteria | Examples | # Genes | Percent |
|---|---|---|---|---|
| Cell wall and development | Associated with cell wall structure, meristem, embryogenesis, desiccation, seed maturation | Cellulase, expansin, extension, HPRG/PRP, LHY, NAM, pectate lyase, pectinesterase, SAH7 | 144 | 3.70 |
| Cytoskeleton | Associated with microtubules and actin | Actin, tubulin, TUBBY, actin binding, myosin | 56 | 1.44 |
| Defense related | Pathogenesis-related (PR) proteins, protease inhibitors, antimicrobial, elicitor induced, apoptosis or HR related, *R* gene homologs | Beta-glucanase, chitinase, metallothioneins, NPR1, PR proteins, SNAKIN, HIN1-like, BAX inhibitor, HSR203J-like, DAD1, LSD1, NDR1, EDS1, Pto interacting, MLO like | 137 | 3.52 |
| DNA / RNA | DNA or RNA binding, DNA or RNA processing, nuclear organization, cell cycle, DNA repair | Ankyrin-like, helicases, histones, nucleases, topoisomerases, transcription factors | 301 | 7.72 |
| Energy | Energy acquisition or production, photosynthesis light reactions, ATP-related | ATP synthases, chlorophylls, photosystem centers, cytochromes, ferredoxin, plastocyanin, thioredoxin | 148 | 3.80 |
| Fatty acid | Fatty acid metabolism | Acetyl Co-A synthase and oxidase, lipase, hydrolase | 52 | 1.33 |
| Heat shock | Heat-shock proteins | HSP10, 24, 60, 70, 80, 81, 83, 90, CCH, DNAJ/K | 59 | 1.51 |
| Hormone | Biosynthesis or hormone regulated | ABA responsive, ARG2, ADR12, GH1, ACC oxidase, ethylene receptor, GIP1, GAI-like, 12-Oxophytodienoate reductase | 99 | 2.54 |
| Membrane | Membrane associated, transporters, pores, vesicle associated | Aquaporins, ABC transporters, ion channels, multidrug resistance-associated protein, clathrin, sugar transport | 192 | 4.93 |
| Oxidation | Related to oxidative stress | Alternate oxidase, GSTs, Germin-like, lipoxygenase, peroxidase, catalase | 121 | 3.10 |
| Primary metabolism | Metabolism of sugars, amino acids, and nucleotides | Glycolysis related, TCA cycle, RUBISCO, nucleotide synthesis, amino acid synthesis | 381 | 9.78 |
| Protein | Protein synthesis, modification, and degradation | Ribosomes, re-folding, prenylation, proteolysis | 345 | 8.85 |
| Secondary metabolism | Metabolism of secondary metabolites | CHS, isoflavone-related, pigmentation, alkaloids, lignins | 155 | 3.98 |
| Senescence | Associated with senescence | Beta-galactosidase, SAG101, ripening-associated protein | 28 | 0.72 |
| Signaling | Signal transduction related | Kinases, phosphatases, GTP binding, calcium associated, inositol-related, 14-3-3 proteins | 297 | 7.62 |
| Stress | Stress related, but unknown function | ERD3, SALI3, SAM22, B2 protein, salt induced, cold induced, wound induced | 62 | 1.59 |
| Miscellaneous | Does not fit neatly into any of the above categories | Nodulin, P450 | 238 | 6.11 |
| No hits | No significant hits in sequence databases | | 378 | 9.70 |
| Unknown | Matched a hypothetical or unknown gene | | 704 | 18.07 |
| Total | | | 3,897 | 100.00 |

reverse transcriptase enzyme) were also included for each sample. cDNA was then quantified by PCR. Primers were designed using Primer Express 2.0 software (Applied Biosystems, Foster City, CA, U.S.A.). PCR reactions were carried out in a total volume of 25 µl containing 0.2 µM of each primer (forward and reverse), 1× SYBR green PCR master mix (Applied Biosystems), and 5 µl of cDNA template. Reactions were amplified in an ABI PRISM 7900HT (Applied Biosystems) as follows: 50°C for 2 min, 95°C for 10 min, followed by 40 cycles of 95°C for 15 s and 59°C for 1 min. A soybean β-actin (AW350943) was used as internal standard to normalize the small difference in template amounts, with the forward primer 5′-CAATCCCAAGGCCAACAGA-3′ and reverse primer 5′-ATGGCAGGCACATTGAAAGTC-3′. This actin control was chosen based on microarray experiments that identified this gene as one that did not vary significantly during either the R or S treatments. All reactions were conducted in triplicate. Quantification was based on a Ct value, which is the PCR cycle number when reaction exceeds a threshold value that is arbitrarily set in the exponential phase of reaction fluorescence. The specificity of the primers was validated by the dissociation curves after the QRT-PCR.

**Chlorophyll fluorescence measurements.**

Chlorophyll fluorescence measurements were collected, using an imaging chlorophyll fluorometer (Walz Imaging PAM, Walz GmbH, Effeltrich, Germany). The area viewed by the fluorometer (2 × 3 cm) was illuminated with 93 µmol $m^{-2}s^{-1}$ proton flux density (PFD) (blue). Chlorophyll fluorescence parameters were measured under steady-state light-adapted conditions. The minimum fluorescence in the light-adapted state (F′) was measured with the measuring pulse from the fluorometer (Baker et al. 2001), using an intensity of 5 and camera gain of 7 (instrument settings). An image of the maximum fluorescence ($F_m'$) was collected following a 1-s saturating pulse (approximately 2,500 µmol $m^{-2}s^{-1}$ PFD). The $\Phi_{PSII}$ was calculated as the quotient ($F_m' - F'/F_m'$) (Baker et al. 2001; Oxborough 2004). At a given incident irradiance and leaf absorbance, $\Phi_{PSII}$ is directly proportional to the rate of electron transport through PSII reaction centers (Genty et al. 1989; Oxborough 2004; Rolfe and Scholes 1995). To determine the operational status of PSII reaction centers, dark-adapted measurements were performed on infected plants 24 hpi, after an 8-h dark period. Images of the minimum ($F_0$) and maximum ($F_m$) fluorescence yield in the dark were collected similarly to the light-adapted measurements. The maximum quantum efficiency of PSII in the dark-adapted state ($F_v/F_m$,) was calculated as ($F_m - F_0$)/$F_m$ (Baker et al. 2001; Oxborough 2004). Following long periods of dark treatment a nearly complete reversal of nonphotochemical quenching can be achieved, thus the value of $F_v/F_m$ is only influenced by the photochemical status of PSII reaction centers. Decreases in this parameter can then be interpreted as decreases in the rate constant for photochemistry ($k_P$), thus direct damage of PSII reaction centers (Oxborough 2004).

## ACKNOWLEDGMENTS

The authors thank K. Lambert for training and use of the QRT-PCR analysis equipment and R. Innes, Indiana University, Bloomington for the *P. syringae* pv. *glycinea* strains. We also thank C. Whitfield and R. Innes for advice and stimulating discussions. This work was financed by a grant from the University of Illinois Soybean Disease Biotechnology Center and the United State Department of Agriculture (USDA)-Agriculture Research Service Current Research Information System 3611-21000-018-00D. Mention of trade names or commercial products in this publication is solely for the purpose of providing specific information and does not imply recommendation or endorsement by the USDA.

## LITERATURE CITED

Aharon, R., Shahak, Y., Wininger, S., Bendov, R., Kapulnik, Y., and Galili, G. 2003. Overexpression of a plasma membrane aquaporin in transgenic tobacco improves plant vigor under favorable growth conditions but not under drought or salt stress. Plant Cell 15:439-447.

Allen, L. J., MacGregor, K. B., Koop, R. S., Bruce, D. H., Karner, J., and Brown, A. W. 1999. The relationship between photosynthesis and a mastoparan-induced hypersensitive response in isolated mesophyll cells. Plant Physiol. 119:1233-1241.

Ashfield, T., Keen, N. T., Buzzell, R. I., and Innes, R. W. 1995. Soybean resistance genes specific for different *Pseudomonas syringae* avirulence genes are allelic, or closely linked, at the RPG1 locus. Genetics 141:1597-1604.

Ashfield, T., Ong, L. E., Nobuta, K., Schneider, C. M., and Innes, R. W. 2004. Convergent evolution of disease resistance gene specificity in two flowering plant families. Plant Cell 16:309-318.

Baker, N. R., Oxborough, K., Lawson, T., and Morison, J. I. L. 2001. High resolution imaging of photosynthetic activities of tissues, cells and chloroplasts in leaves. J. Exp. Biol. 52:615-621.

Barber, J., and Andersson, B. 1992. Too much of a good thing: Light can be bad for photosynthesis. Trends Biochem Sci. 17:61-6.

Bendahmane, A., Kanyuka, K., and Baulcombe, D. C. 1999. The *Rx* gene from potato controls separate virus resistance and cell death responses. Plant Cell 11:781-92.

Benjamini, Y., and Hochberg, Y. 1995. Controlling the false discovery rate: A practical and powerful approach to multiple testing. J. Royal Statistical Society Series B. 57:289-300.

Bonas, U., and Lahaye, T. 2002. Plant disease resistance triggered by pathogen-derived molecules: Refined models of specific recognition. Curr. Opin. Microbiol. 5:44-50.

Chen, Z., Kloek, A. P., Cuzick, A., Moeder, W., Tang, D., Innes, R. W., Klessig, D. F., McDowell, J. M., and Kunkel, B. N. 2004. The *Pseudomonas syringae* type III effector AvrRpt2 functions downstream or independently of SA to promote virulence on *Arabidopsis thaliana*. Plant J. 37:494-504.

Clough, S. J., Fengler, K. A., Yu, I. C., Lippok, B., Smith, R. K., Jr., and Bent, A. F. 2000. The *Arabidopsis dnd1* "defense, no death" gene encodes a mutated cyclic nucleotide-gated ion channel. Proc. Natl. Acad. Sci. U.S.A. 97:9323-8.

Deák, M., Horváth, G. V., Davletova, S., Török, K., Sass, L., Vass, I., Barna, B., Király, Z., and Dudits, D. 1999. Plants ectopically expressing the ironbinding protein, ferritin, are tolerant to oxidative damage and pathogens. Nature Biotechnol. 17:192-196.

Doke, N. 1983. Involvement of superoxide anion generation in the hypersensitive response of potato tuber tissues to infection with an incompatible race of *Phytophthora infestans* and the hyphal wall components. Physiol. Plant Pathol. 23:345-357.

Foyer, C. H., and Noctor, G. 2003. Redox sensing and signaling associated with reactive oxygen in chloroplasts, peroxisomes and mitochondria. Physiol. Plant 119:355-364.

Foyer, C. H., and Noctor, G. 2005. Redox homeostasis and antioxidant signaling: A metabolic interface between stress perception and physiological responses. Plant Cell 17:1866-1875.

Genty, B., Briantais, J. M., and Baker, N. R. 1989. The relationship between the quantum yield of photosynthetic electron-transport and quenching of chlorophyll fluorescence. Biochim. Biophys. Acta. 990:87-92.

Gray, J., Close, P. S., Briggs, S. P., and Johal, G. S. 1997. A novel suppressor of cell death in plants encoded by the *Lls1* gene of maize. Cell 89:25-31.

Greenberg, J. T., and Ausubel, F. M. 1993. Arabidopsis mutants compromised for the control of cellular damage during pathogenesis and aging. Plant J. 4:327-41.

Hammond-Kosack, K., and Jones, J. D. G. 2000. Responses to plant pathogens. Pages 1102-1156 in: Biochemistry and Molecular Biology of Plants. B. B. Buchanan, W. Gruissem and R. L. Jones, eds. American Society of Plant Physiologists, Rockville, MD, U.S.A.

Hegde, P., Qi, R., Abernathy, K., Gay, C., Dharap, S., Gaspard, R., Hughes, J. E., Snesrud, E., Lee, N., and Quackenbush, J. 2000. A concise guide to cDNA microarray analysis. BioTechniques 29:548-562.

Jabs, T. 1999. Reactive oxygen intermediates as mediators of programmed cell death in plants and animals. Biochem. Pharmacol. 57:231-245.

Jamir, Y., Guo, M., Oh, H.-S., Petnicki-Ocwieja, T., Chen, S., Tang, X., Dickman, M. B., Collmer, A., and Alfano, J. R. 2004. Identification of *Pseudomonas syringae* type III effectors that can suppress programmed cell death in plants and yeast. Plant J. 37:554-565.

Kearney, B., and Staskawicz, B. J. 1990. Widespread distribution and fitness contribution of *Xanthomonas campestris* avirulence gene *avrBs2*. Nature 346:385-386.

Keppler, L. D., and Baker, C. J. 1989. $O_2$- initiated lipid peroxidation in a

bacteria-induced hypersensitive reaction in tobacco cell suspensions. Phytopathology 79:555-562.
Keppler, L. D., and Novacky, A. 1987. The initiation of membrane lipid peroxidation during bacteria-induced hypersensitive reaction. Physiol. Mol. Plant Pathol. 30:233-245.
Kerr, M. K., Martin, M., and Churchill, G. A. 2000. Analysis of variance for gene expression microarray data. J. Comput. Biol. 7:819-837.
Koch, E., Meier, B. M., Eiben, H. G., and Slusarenko, A. 1992. A lipoxygenase from leaves of tomato (Lycopersicon esculentum Mill.) is induced in response to plant pathogenic Pseudomonads. Plant Physiol. 99:571-576.
Laloi, C., Apel, K., and Danon, A. 2004. Reactive oxygen signaling: The latest news. Curr. Opin. Plant Biol. 7:323-328.
Lamb, C., and Dixon, R. A. 1997. The oxidative burst in plant disease resistance. Annu. Rev. Plant Physiol. Plant Mol. Biol. 48:251-275.
Lawlor, D. W. 2002. Limitation to photosynthesis in water-stressed leaves: Stomata vs. metabolism and the role of ATP. Ann. Bot. 89:871-885.
Levine, A., Tenhaken, R., Dixon, R., and Lamb, C. 1994. $H_2O_2$ from the oxidative burst orchestrates the plant hypersensitive disease response. Cell 79:583-593.
Lincoln, J. E., Richael, C., Overduin, B., Smith, K., Bostock, R., and Gilchrist, D. G. 2002. Expression of the antiapoptotic baculovirus p35 gene in tomato blocks programmed cell death and provides broad-spectrum resistance to disease. Proc. Natl. Acad. Sci. U.S.A. 99:15217-15221.
Ludwig, A., and Tenhaken, R. 2000. Defence gene expression in soybean is linked to the status of the cell death program. Plant Mol. Biol. 44:209-218.
Ludwig, A., and Tenhaken, R. 2001. A new cell located N-rich protein is strongly induced during the hypersensitive response in *Glycine max* L. Eur. J. Plant Pathol. 107:323-336.
Mahalingam, R., and Fedoroff, N. 2003. Stress response, cell death and signaling: The many faces of reactive oxygen species. Physiol. Plant. 119:56-68.
Matsumura, H., Reich, S., Ito, A., Saitoh, H., Kamoun, S., Winter, P., Kahl, G., Reuter, M., Kruger, D. H., and Terauchi, R. 2003. Gene expression analysis of plant host-pathogen interactions by SuperSAGE. Proc. Natl. Acad. Sci. U.S.A. 100:15718-15723.
Moy, P., Qutob, D., Chapman, B. P., Atkinson, I., and Gijzen, M. 2004. Patterns of gene expression upon infection of soybean plants by *Phytophthora sojae*. Mol. Plant-Microbe Interact. 17:1051-1062.
Napoli, C., and Staskawicz, B. 1987. Molecular characterization and nucleic acid sequence of an avirulence gene from race 6 of *Pseudomonas syringae* pv. *glycinea*. J. Bacteriol. 169:572-578.
Oxborough, K. 2004. Imaging of chlorophyll a fluorescence: Theoretical and practical aspects of an emerging technique for the monitoring of photosynthetic performance. J. Exp. Bot. 55:1195-1205.
Pfannschmidt, T. 2003. Chloroplast redox signals: How photosynthesis controls its own genes. Trends Plant Sci. 8:33-41.
Pruzinska, A., Tanner, G., Anders, I., Roca, M., and Hortensteiner, S. 2003. Chlorophyll breakdown: Pheophorbide *a* oxidase is a Rieske-type iron-sulfur protein, encoded by the *accelerated cell death 1* gene. Proc. Natl. Acad. Sci. 100:15259-15264.
Quirino, B. F., and Bent, A. F. 2003. Deciphering host resistance and pathogen virulence: The *Arabidopsis/Pseudomonas* interaction as a model. Mol. Plant Pathol. 4:517-530.
Rolfe, S. A., and Scholes, J. D. 1995. Quantitative imaging of chlorophyll fluorescence. New Phytol. 131:69-79.
Rooney, H. C. E., van't Klooster, J. W., van der Hoorn, R. A. L., Joosten, M. H. A. J., Jones, J. D. G., and de Wit, P. J. G. M. 2005. Cladosporium Avr2 inhibits tomato Rcr3 protease required for *Cf-2*-dependent disease resistance. Science. 308:1783-1786.
Rusterucci, C., Montillet, J. L., Agnel, J. P., Battesti, C., Alonso, B., Knoll, A., Bessoule, J. J., Etienne, P., Suty, L., Blein, J. P., and Triantaphylides, C. 1999. Involvement of lipoxygenase-dependent production of fatty acid hydroperoxides in the development of the hypersensitive cell death induced by crytogein on tobacco leaves. J. Biol. Chem. 274:36446-36455.
Scheel, D. 1998. Resistance response physiology and signal transduction. Curr. Opin. Plant Biol. 1:305-310.
Scheideler, M., Schlaich, N. L., Fellenberg, K., Beissbarth, T., Hauser, N. C., Vingron, M., Slusarenko, A. J., and Hoheisel, J. D. 2002. Monitoring the switch from housekeeping to pathogen defense metabolism in *Arabidopsis thaliana* using cDNA arrays. J. Biol. Chem. 277:10555-10561.
Seehaus, K., and Tenhaken, R. 1998. Cloning of genes by mRNA differential display induced during the hypersensitive reaction of soybean after inoculation with *Pseudomonas syringae* pv. *glycinea*. Plant Mol. Biol. 38:1225-1234.
Seo, S., Okamoto, M., Iwai, T., Iwano, M., Fukui, K., Isogai, A., Nakajima, N., and Ohashi, Y. 2000. Reduced levels of chloroplast FtsH protein in tobacco mosaic virus-infected tobacco leaves accelerate the hypersensitive reaction. Plant Cell 12:917-932.
Shoemaker, R., Keim, P., Vodkin, L., Retzel, E., Clifton, S. W., Waterston, R., Smoller, D., Coryell, V., Khanna, A., Erpelding, J., Gai, X. W., Brendel, V., Raph-Schmidt, C., Shoop, E. G., Vielweber, C. J., Schmatz, M., Pape, D., Bowers, Y., Theising, B., Martin, J., Dante, M., Wylie, T., and Granger, C. 2002. A compilation of soybean ESTs: Generation and analysis. Genome 45:329-338.
Smirnoff, N., and Wheeler, G. L. 2000. Ascorbic acid in plants: Biosynthesis and function. Crit Rev Biochem Mol Biol. 35:291-314.
Spetea, C., Hundal, T., Lohmann, F., and Andersson, B. 1999. GTP bound to chloroplast thylakoid membranes is required for light-induced, multienzyme degradation of the photosystem II D1 protein. Proc. Natl. Acad. Sci. U.S.A. 96:6547-6552.
Staskawicz, B., Dahlbeck, D., Keen, N., and Napoli, C. 1987. Molecular characterization of cloned avirulence genes from race 0 and race 1 of *Pseudomonas syringae* pv. *glycinea*. J. Bacteriol. 169:5789-5794.
Staskawicz, B. J., Dahlbeck, D., and Keen, N. T. 1984. Cloned avirulence gene of *Pseudomonas syringae* pv. *glycinea* determined race-specific incompatibility on *Glycine max* (L.) Merr. Proc. Natl. Acad. Sci. U.S.A. 81:6024-6028.
Takahashi, H., Chen, Z., Du, H., Liu, Y., and Klessing, D. F. 1997. Development of necrosis and activation of disease resistance in transgenic tobacco plants with severely reduced catalase levels. Plant J. 11:993-1005.
Tamaki, S., Dahlbeck, D., Staskawicz, B., and Keen, N. T. 1988. Characterization and expression of two avirulence genes cloned from *Pseudomonas syringae* pv. *glycinea*. J. Bacteriol. 170:4846-4854.
Tao, Y., Xie, Z., Chen, W., Glazebrook, J., Chang, H.-S., Han, B., Zhu, T., Zou, G., and Katagiri, F. 2003. Quantitative nature of Arabidopsis responses during compatible and incompatible interactions with the bacterial pathogen *Pseudomonas syringae*. Plant Cell 15:317-330.
United States Department of Agriculture. 2001. Soy stats: A reference guide to important soybean facts and figures. American Soybean Association, United States Department of Agriculture, St. Louis.
Vandenabeele, S., Van Der Kelen, K., Dat, J., Gadjev, I., Boonefaes, T., Morsa, S., Rottiers, P., Slooten, L., Van Montagu, M., Zabeau, M., Inze, D., and Van Breusegem, F. 2003. A comprehensive analysis of hydrogen peroxide-induced gene expression in tobacco. Proc. Natl. Acad. Sci. U.S.A. 100:16113-16118.
Vivian, A., and Gibbon, M. J. 1997. Avirulence genes in plant-pathogenic bacteria: Signals or weapons? Microbiology 143:693-704.
Vodkin, L. O., Khanna, A., Shealy, R. T., Clough, S. J., Gonzales, D. O., Philip, R., Zabala, G. C., Thibaud-Nissen, F., Sidarous, M., Stromvik, M. V., Shoop, E. G., Schmidt, C., Retzel, E., Erpelding, J., Shoemaker, R. C., Rodrizues-Huete, A. M., Polacco, J. C., Coryell, V., Keim, P., Gong, G., Lui, L., Pardinas, J. L., and Schweitzer, P. 2004. Microarrays for global expression constructed with a low redundancy set of 27,500 sequenced cDNAs representing an array of developmental stages and physiological conditions of the soybean plant. BMC Genomics 5:73.
Wan, J., Dunning, F. M., and Bent, A. F. 2002. Probing plant-pathogen interactions and downstream signaling using DNA microarrays. Funct. Integr. Genomics. 2:259-273.
Winkel-Shirley, B. 2001. Flavonoid biosynthesis. A colorful model for genetics, biochemistry, cell biology, and biotechnology. Plant Physiol. 126:485-93.
Wright, C. A., and Beattie, G. A. 2004. *Pseudomonas syringae* pv. *tomato* cells encounter inhibitory levels of water stress during the hypersensitive response of *Arabidopsis thaliana*. Proc. Natl. Acad. Sci. U.S.A. 101:3269-3274.
Wu, H., Kerr, M. K., Cui, X., and Churchill, G. A. 2003. MAANOVA: A software package for the analysis of spotted cDNA microarray experiments. Pages 313-341 in: The Analysis of Gene Expression Data: Methods and Softwares. G. Parmigiani, E. S. Garrett, R. A. Irizarry and S. L. Zeger, eds. Springer, New York.
Yu, I.-C., Parker, J., and Bent, A. F. 1998. Disease resistance without the hypersensitive response in *Arabidopsis dnd1* mutant. Proc. Natl. Acad. Sci. U.S.A. 95:7819-7824.
Zhang, C., Gutsche, A. T., and Shapiro, A. D. 2004. Feedback control of the *Arabidopsis* hypersensitive response. Mol. Plant-Microbe Interact. 17:357-365.

## AUTHOR-RECOMMENDED INTERNET RESOURCES

Biogenetic Services, Inc.: www.biogeneticservices.com
American Type Culture Collection: www.atcc.org
The Institute for Genomic Research (TIGR) plant gene indices website: www.tigr.org/tbd/tgi/index.shtml